



AFRL-RX-TY-TR-2012-0073-01

## **HUMANLIKE ARTICULATED ROBOTIC HEADFORM TO REPLACE HUMAN VOLUNTEERS IN RESPIRATOR FIT TESTING**

---

Joseph Wander  
Airbase Technologies Division  
Air Force Research Laboratory  
139 Barnes Drive, Suite 2  
Tyndall Air Force Base, FL 32403-5323

David Hanson and Richard Margoli}  
Hanson Robotics  
1201 Creekfield Drive  
Plano, TX 75075-4004

Contract No. FA4819-11-C-0012

December 2012

**DISTRIBUTION A.** Approved for public release; distribution unlimited.  
88ABW-2013-0479, 1 February 2013.

**AIR FORCE RESEARCH LABORATORY  
MATERIALS AND MANUFACTURING DIRECTORATE**

## **DISCLAIMER**

Reference herein to any specific commercial product, process, or service by trade name, trademark, manufacturer, or otherwise does not constitute or imply its endorsement, recommendation, or approval by the United States Air Force. The views and opinions of authors expressed herein do not necessarily state or reflect those of the United States Air Force.

This report was prepared as an account of work sponsored by the Biomedical Research and Development Authority (BARDA), U.S. Department of Health and Human Services and contracted and managed by the United States Air Force. Neither BARDA nor the United States Air Force, nor any of their employees, makes any warranty, expressed or implied, or assumes any legal liability or responsibility for the accuracy, completeness, or usefulness of any information, apparatus, product, or process disclosed, or represents that its use would not infringe privately owned rights.

## NOTICE AND SIGNATURE PAGE

Using Government drawings, specifications, or other data included in this document for any purpose other than Government procurement does not in any way obligate the U.S. Government. The fact that the Government formulated or supplied the drawings, specifications, or other data does not license the holder or any other person or corporation; or convey any rights or permission to manufacture, use, or sell any patented invention that may relate to them.

This report was cleared for public release by the 88th Air Base Wing Public Affairs Office at Wright Patterson Air Force Base, Ohio available to the general public, including foreign nationals. Copies may be obtained from the Defense Technical Information Center (DTIC) (<http://www.dtic.mil>).

AFRL-RX-TY-TR-2012-0073-01 HAS BEEN REVIEWED AND IS APPROVED FOR PUBLICATION IN ACCORDANCE WITH ASSIGNED DISTRIBUTION STATEMENT.

WANDER.JOSEP  
H.D.1230231660

Digitally signed by  
WANDER.JOSEPH.D.1230231660  
DN: c=US, o=U.S. Government, ou=DoD, ou=PKI,  
ou=USAF, cn=WANDER.JOSEPH.D.1230231660  
Date: 2013.01.24 14:25:40 -0600

---

JOSEPH D. WANDER, PhD  
Work Unit Manager

HENLEY.MICHAEL.V.1231823332

Digitally signed by HENLEY.MICHAEL.V.1231823332  
DN: c=US, o=U.S. Government, ou=DoD, ou=PKI,  
ou=USAF, cn=HENLEY.MICHAEL.V.1231823332  
Date: 2013.01.09 16:57:39 -0600

---

MICHAEL V. HENLEY, DR-IV  
Chief, Airbase Sciences Branch

RHODES.ALBERT.N.III.1175488622

Digitally signed by  
RHODES.ALBERT.N.III.1175488622  
DN: c=US, o=U.S. Government, ou=DoD, ou=PKI,  
ou=USAF, cn=RHODES.ALBERT.N.III.1175488622  
Date: 2013.01.31 08:16:50 -0600

---

ALBERT N. RHODES, PhD  
Chief, Airbase Technologies Division

This report is published in the interest of scientific and technical information exchange, and its publication does not constitute the Government's approval or disapproval of its ideas or findings.

**REPORT DOCUMENTATION PAGE**

*Form Approved  
OMB No. 0704-0188*

The public reporting burden for this collection of information is estimated to average 1 hour per response, including the time for reviewing instructions, searching existing data sources, gathering and maintaining the data needed, and completing and reviewing the collection of information. Send comments regarding this burden estimate or any other aspect of this collection of information, including suggestions for reducing the burden, to Department of Defense, Washington Headquarters Services, Directorate for Information Operations and Reports (0704-0188), 1215 Jefferson Davis Highway, Suite 1204, Arlington, VA 22202-4302. Respondents should be aware that notwithstanding any other provision of law, no person shall be subject to any penalty for failing to comply with a collection of information if it does not display a currently valid OMB control number.

**PLEASE DO NOT RETURN YOUR FORM TO THE ABOVE ADDRESS.**

<b>1. REPORT DATE (DD-MM-YYYY)</b> 01-DEC-2012	<b>2. REPORT TYPE</b> Final Technical Report	<b>3. DATES COVERED (From - To)</b> 11-APR-2011 -- 10-APR-2012
---	---	---

<b>4. TITLE AND SUBTITLE</b> Humanlike Articulate Robotic Headform to Replace Human Volunteers in Respirator Fit Testing	<b>5a. CONTRACT NUMBER</b> FA4819-11-C-0012
	<b>5b. GRANT NUMBER</b>
	<b>5c. PROGRAM ELEMENT NUMBER</b> 0909999F

<b>6. AUTHOR(S)</b> ^Wander, Joseph; *Hanson, David; *Margolin, Richard	<b>5d. PROJECT NUMBER</b> GOVT
	<b>5e. TASK NUMBER</b> L0
	<b>5f. WORK UNIT NUMBER</b> X0CH (QL102025)

<b>7. PERFORMING ORGANIZATION NAME(S) AND ADDRESS(ES)</b> *Hanson Robotics 1201 Creekfield Drive Plano, TX 75075-4004	<b>8. PERFORMING ORGANIZATION REPORT NUMBER</b>
--	---

<b>9. SPONSORING/MONITORING AGENCY NAME(S) AND ADDRESS(ES)</b> ^Air Force Research Laboratory Materials and Manufacturing Directorate Airbase Technologies Division 139 Barnes Drive, Suite 2 Tyndall Air Force Base, FL 32403-5323	<b>10. SPONSOR/MONITOR'S ACRONYM(S)</b> AFRL/RXQL
	<b>11. SPONSOR/MONITOR'S REPORT NUMBER(S)</b> AFRL-RX-TY-TR-2012-0073-01

**12. DISTRIBUTION/AVAILABILITY STATEMENT**  
Distribution A. Approved for public release; distribution unlimited.

**13. SUPPLEMENTARY NOTES**  
Ref Public Affairs case number 88ABW-2013-0479, 1 February 2013. Document contains color images.

**14. ABSTRACT**  
In this era of competent materials and fabrication for air filtration the factor dictating the protection factor (ratio of concentration outside to inside the respirator) is unfiltered inward leakage. Respirator testing using humans is constrained by the requirement for advance approval of the protocol by a human use committee, by the diversity and caprices of the subjects used in testing, by factors such as fatigue and illness, and by health hazards of aerosol challenges. Hanson Robotics has designed and built a robotic headform with dimensions matching those of the medium headform identified from a NIOSH wearers panel. The polyurethane skull form and polydimethylsiloxane artificial skin covering (Frubber) also accurately reproduce skin thicknesses measured for a panel of male Caucasians aged 19 -22 and provide a good simulation of the gross surface texture of human skin and its elastic response to touch. An initial static test of fit of seven models of N95 respirators to a static prototype prepared from similar materials in the same dimensions showed a typical scatter of measured fit factors (FFs) after donning, and an average FF of slightly more than 200 in a second series of donnings in which a leak check was used to exclude samples for which FF was <100, showing that the headform does closely resemble a human head in the NIOSH medium size window. Statistical validation that this similarity constitutes functional equivalence is underway.

**15. SUBJECT TERMS**  
artificial skin, face seal, fit test, Frubber, headform, leakage, respirator, robot

<b>16. SECURITY CLASSIFICATION OF:</b>			<b>17. LIMITATION OF ABSTRACT</b> SAR	<b>18. NUMBER OF PAGES</b> 31	<b>19a. NAME OF RESPONSIBLE PERSON</b> Joseph D. Wander
<b>a. REPORT</b> U	<b>b. ABSTRACT</b> U	<b>c. THIS PAGE</b> U			<b>19b. TELEPHONE NUMBER (Include area code)</b> 850 283-6240

Reset

## TABLE OF CONTENTS

LIST OF FIGURES .....	ii
ACKNOWLEDGMENTS .....	iii
1. EXECUTIVE SUMMARY .....	1
2. INTRODUCTION .....	3
3. STATIC HEADFORM .....	6
3.1. Headform Design Specifications .....	6
3.2. Headform Construction and Skin Covering.....	6
3.2.1. Background .....	6
4. ARTICULATED HEADFORM .....	13
4.1. Design Changes and Component Assembly .....	13
4.1.1. Adjustments after Initial Headform Testing .....	13
4.1.2. Evolution of Skull Design.....	13
4.1.3. Software and Integration.....	20
5. DISCUSSION .....	21
5.1. Static Headform .....	21
5.2. Articulated Headform .....	21
5.3. General.....	22
5.4. Conclusions.....	23
6. REFERENCES .....	24
LIST OF SYMBOLS, ABBREVIATIONS AND ACRONYMS .....	28

## LIST OF FIGURES

	<b>Page</b>
Figure 1. 2010 Embodiment of Diego-San Robot, Which Uses Frubber™ to Create Humanlike Facial Expressions in a Mobile Robot Platform to Study Human–robot Interactions.....	7
Figure 2. Scanning Electron Micrographs, Showing Increased Heirchical Porosity in the Rightmost Sample. (Courtesy of NSF funding and Richland College in Dallas).....	8
Figure 3. NIOSH Standard Medium Headform.....	8
Figure 4. NIOSH Medium Headform with Additional Details.....	9
Figure 5. Mold of the Detailed NIOSH Medium Headform.....	9
Figure 6. Locations of Landmarks of Variable Thicknesses of Human Facial Soft Tissue <sup>[58]</sup> .....	10
Figure 7. 3D Design Study of Facial Landmark Thickness.....	10
Figure 8. Face Mold Negative Form with Tissue Thickness Markers Emplaced.....	11
Figure 9. Reverse Forensic Facial Reconstruction Used to Generate Anatomically Accurate Skull Form .....	11
Figure 10. Laser Scan of the Skull, Showing Registration Features .....	12
Figure 11. Static Headform with Anatomically Accurate Facial “Skin” Thicknesses .....	12
Figure 12. NIOSH Surface Form Evaluation, Correlated with the NIOSH Medium File.....	13
Figure 13. Brushless Servo Selected for Implementation.....	13
Figure 14. Skull Forms, As Originally Proposed (left) and Revised to Emplace the Brushless Servos (right) .....	14
Figure 15. Second Redesign of Articulated Skull Form .....	14
Figure 16. Mechanical Designs, Showing Gasket-sealed Maintenance Access Panel, Neck Integration and Initial Servo Configuration.....	15
Figure 17. Expression Anchor Implementations .....	16
Figure 18. Articulated Skull Form (left) and Articulated Support (Neck)(right) .....	16
Figure 19. Initial (left) and Improved Articulated Skin Implementations .....	17
Figure 20. Design Sketch of Oral Cavity Manifold.....	17
Figure 21. Oral Cavity Manifold; Side (left) and Front Views (center) Closed, and Front View Open (right).....	18
Figure 22. Side (left) and Rear Views (right) of Trajectory of Breathing Tube.....	18
Figure 23. Manifold–Breathing Tube Joint; Top View of Connection (left) and Rear View Showing Breathing Tube Installed.....	19
Figure 24. Rear View of Skull Form Showing Components Surrounding Manifold–Breathing Tube Joint.....	19
Figure 25. Original (left) and Redesigned Neck Structures (center, right).....	20
Figure 26. Distribution of Geometric Mean Fit Factors (n = 112 Data Points) <sup>[60]</sup> .....	21

## **ACKNOWLEDGMENTS**

The authors sincerely thank the following for their support and contributions:  
William Hicks; Elaine Hanson; John Hatch; Amanda Hanson; Mike McDonald and Brian Heimbuch, ARA; Bob Nichols, UTC; Michael Bergman and Ziqing Zhuang, NIOSH-NPPTL; Louis Schwartz, Paulette Demont, Peter Parsinen, Joshua Jach, Jim Ash, Leslie Richardson, and Hanson RoboKind LLC.

## 1. EXECUTIVE SUMMARY

The testing of individual respiratory protection (IRP) devices is now accomplished with panels of human wearers. Historical attempts to simulate the human face and head have been unsuccessful for a variety of reasons that include imprecision in reproduction of facial dimensions and unrepresentative textures of the surfaces applied to headforms used. Hanson Robotics has designed and built two headforms, one static and one articulated and actuated to accurately reproduce the facial gestures and movements of a human whose anthropometric dimensions fall within the window identified by the National Institute for Occupational Safety and Health (NIOSH) as a short/wide headform and just outside the window for a medium headform.

The static headform was built first as a prototype to work out many of the details of material composition and configuration. Skin thickness was specified to reproduce a set of ultrasound measurements reported for a panel of young adult male Caucasians. This was accomplished by an inverse forensic reconstruction technique in which a mold of the NIOSH medium headform was cast and clay was applied to the (negative) surface of the mold in a layer whose local thicknesses matched the measured skin thickness. Pins inserted into the negative surface guided the clay thickness. The skull form was then cast to the clay negative surface, and used subsequently as a complementary mold surface to cast the polydimethylsiloxane (PDMS) skin (Frubber™) with anatomically accurate thickness. For this the molds were oriented with locating pins, and for assembly the skull form and skin included locating dimples in areas noncritical to respirator fitting.

A simplified fit test under static conditions at NIOSH showed this head to achieve fit factors (FFs) slightly better than average values measured for the complete protocol—which includes movement—a result we considered completely successful for the first stage, and a process of design refinement and construction of an articulated, robotic headform in the same dimensions was undertaken. Hanson's history of robot development was invaluable in this exercise but it still involved extensive research and development in several areas. Feedback that the skin thickness near the top of the head was a bit too thin led to a jig that has since been used to verify dimensions during assembly.

Incorporation of anchors used to connect the skin through cables to individual servos caused moderate (5%) swelling of the PDMS after removal from the molds. A series of washing and baking steps restored the original dimension but the texture of the skin was unsatisfactory, which triggered several cycles of reformulation and casting that led to a Frubber™ composition that exhibits both stable dimensions and appropriate mechanical properties. Routing of the breathing tube down through the throat was precluded by the array of components in the lower jaw used to drive lower facial expressions and movements, a problem aggravated by an increase in its inside diameter from  $\frac{3}{4}$  in to 1 in. The solution selected was to route the air up the front of the face, over the top and down the back of the head and thence down the back of the neck.

The stiffest challenge was achieving an airtight seal around the electronic and mechanical components enclosed in the skull form from aerosolized water and salts in both the external environment (AFRL's exposure chamber) and the breathing tube, through which the same aerosol was drawn through a test respirator and eventually delivered to sampling equipment.

After several false starts this was accomplished by inverting the physiology of the oral cavity in an elastomeric casting that was sealed with an adhesive to the lips of the Frubber™ skin and that engaged the breathing tube on its upper face.

The software controlling movement was upgraded to include sensing and reporting errors in motor activity. Instructions for user interaction with the software are included in a companion report.<sup>[60]</sup> Fixed attachment points and locating dimples were again sited in locations noncritical to mask fit, to ensure accurate registration of the skin with the skull form during assembly and in use. Teeth were deleted from the final design as unnecessary to the purpose of the headform. The first articulated headform was delivered in September 2012. Two more headforms—one of each type—are being prepared for delivery.

Initial fit testing results suggest that the static headform accurately reproduces the dimensions and textures of the NIOSH medium head. The first application targeted is upgrading N95 respirator certification under 42 CFR 84 to a basis of protection factor (PF) rather than particle exclusion by the medium; however, markets to support respirator design, leak testing, use of hazardous challenges and PF measurements during extreme exercise/stress are anticipated.

## 2. INTRODUCTION

The concept of respiratory protection dates to antiquity—Pliny the Elder and Galen, in the first and second centuries A.D., respectively, recommended the use of animal bladders as masks to protect miners from diseases caused by inhalation of asbestos,<sup>[1]</sup> mercury,<sup>[2]</sup> zinc, sulfur and lead dusts.<sup>[3]</sup> Airborne particle weapons—delivering arsenical combustion products—first appeared no later than the 13<sup>th</sup> century in China<sup>[4]</sup> and use of such smokes is reported as early as 1000 B.C. by the Chinese and during the Peloponnesian War.<sup>[5]</sup> As a corollary to an arsenical smoke weapon he proposed for naval warfare, Leonardo da Vinci suggested that a wet, finely woven cloth could protect sailors from the particles<sup>[6]</sup> and, later in the 16th century, Agricola described a broadly similar concept to limit exposure to mining dusts.<sup>[7]</sup>

Practical early respirators completely enclosed the head and either supplied air from a reservoir or scrubbed CO<sub>2</sub> in a rebreather.<sup>[8]</sup> The 1848 US patent<sup>[9]</sup> for *Haslett's Lung Protector* describes the first air purifying respirator, inhalation occurring through wet wool and exhalation opening a clapper valve, and Hurd patented a cup-shaped mask in 1879.<sup>[10]</sup> Stenhouse incorporated activated charcoal into a respirator able to capture toxic gases from the air,<sup>[11,12]</sup> to which by 1871 Tyndall<sup>[13]</sup> had added a filter of cotton wool saturated with lime, glycerin, and charcoal—the *fireman's respirator*—a hood that filtered both smoke particles and gases from air.<sup>[14]</sup> During the Second Battle of Ypres,<sup>[15]</sup> Germany institutionalized the use of toxic chemicals as a large-scale weapon by releasing 168 tons of chlorine from high ground onto a 4-mi (6-km) section on the Western Front, killing 6,000 troops by asphyxiation within 10 minutes, and damaging the lungs and the eyes of survivors. An improvised response by Canadian troops, using urine-soaked cloths as primitive respirators to dissolve and neutralize the chlorine vapor, is cited as the first recorded response and defense against chemical attacks using respirators.<sup>[16]</sup>

A second German-engineered device—a filter fabricated from crocidolite asbestos and esparto grass—ushered in the era of high-efficiency particle filters. Reverse engineering of this smoke filter by a Department of Defense (DoD) panel during WWII<sup>[17]</sup> led to the development by the nuclear community of high-efficiency particulate air (HEPA) media to control ~300-nm particles of radioactive iodine.<sup>[18]</sup>

A comprehensive review by Davies<sup>[19]</sup> in 1967 details the evolution of filter theory and validating experimentation that occurred during the preceding 25 years, and laments<sup>[20]</sup> that developers and users of filters did not incorporate these advances in understanding. Davies' review notes Freundlich's recognition<sup>[21]</sup> in 1922 of the dip in the efficiency curve at the crossover from inertial to diffusional capture mechanisms—now called the most-penetrating particle size (MPPS)—and Kaufman's insight<sup>[22]</sup> in 1936 that particle capture becomes more efficient as the filter fiber diameter narrows—*i.e.*, that the pillars of modern theory were in place before WWII. Electrospinning dates to a 1900 patent, so the concept of nanofiber filters—which have lately acquired a measure of interest to the DoD in only the past few years—has been in the literature for more than seven decades. The timing of Kaufman's report is consistent with an obituary<sup>[23]</sup> in which Lushkinov claims that Russian engineers began working on nanofiber air filter media before WWII.

A review by Herris of the coevolution of respirator technology and respiratory protection standards cites firemen—who operate in environments rife with both toxic gases and ultrafine

particles—as the principal targets of respirator developments<sup>[24]</sup> prior to WWI, during which the military significance of respiratory protective gear became clear.<sup>[5]</sup> Respirator certification standards, including 30 CFR 11 and its successor 42 CFR 84,<sup>[25]</sup> and European standards EN 143<sup>[26]</sup> and EN 149,<sup>[27]</sup> specify only the particle removal efficiency of the medium. 29 CFR 1910.134<sup>[28]</sup> includes a requirement for individual quantitative fit testing (QNFT).<sup>[29]</sup>

In QNFT the FF of an individual FFR is defined as the ratio of the concentration of a test agent outside to the concentration inside the device. Individual fit testing is used to assure that tight-fitting respirators provide their expected level of protection.<sup>[30–32]</sup> Studies have demonstrated the importance of fit testing for achieving acceptably large simulated workplace protection factors.<sup>[33,34]</sup> Contaminant inward leakage (IL) into a respirator facepiece has been defined as a combination of leakage through 1) the face seal, 2) the filter element, 3) exhalation valves (for FFRs so equipped) and 4) other sites (e.g., areas at which head straps are connected to the FFR by staples, stitching, etc.)<sup>[35]</sup>; however, facepiece fit has been shown to be the dominant contributor to IL.<sup>[36,37]</sup>

Recognition that protection is limited by the quality of fit has stimulated interest in IL testing of FFRs using viable pathogens; however, no test system existed for performing such tests. Traditionally, IL tests have been performed with human subjects using inert aerosols such as sodium chloride. Static manikin headforms have been used in previous filtration and face seal leakage studies, but they did not simulate head movements or speech, and were usually covered with a thin layer of rubber or plastic that made no attempt to mimic the thickness and properties of human facial tissue (e.g., stretching, wrinkling, and compressibility). Cooper et al. assessed face–seal leakage of an FFR on a static headform covered with a thin film of poly(vinyl chloride) (PVC) plastisol. Using a breathing machine operating at a flow rate of 37 L/min and an aerosol challenge of 1.8- $\mu\text{m}$  monodisperse diisooctyl phthalate they measured face seal leakage of 19%.<sup>[38]</sup> Similarly, face seal leakage of a polydisperse aerosol of corn oil past two models of elastomeric, particle-filtering half-mask respirators fitted to a Sheffield headform and a breathing machine operating at a flow rate of 50 L/min was particle-size dependent but both models showed > 40% leakage for particles < 1  $\mu\text{m}$ .<sup>[39]</sup> Cohen achieved FFs > 1,667 (the Army criterion) for a medium-size U.S. Army M40 full facepiece elastomeric protective mask mounted on a headform with a rubber skin, connected to a breathing machine operating at 30 L/min, and challenged with ambient aerosol.<sup>[40]</sup> Respirators have also been sealed to manikin headforms and then modified with artificial leaks to measure particle leakage<sup>[41–44]</sup>; however, artificial static leaks in respirators sealed to headforms are not representative of leaks into respirators worn by people, which are dynamic and fluctuate in size.<sup>[45–47]</sup>

Respirator test headforms have evolved in recent years. Richardson et al. utilized a silicone polymer skin to perform fit testing of an M40 mask on both static and articulated headforms.<sup>[48]</sup> Operating a breathing machine at 25 L/min they measured FFs of 220–9,300 (geometric mean 1,500) for the static headform and FFs of 8,000–9,000 for head movements but of only 1,000–2,000 for recitation of the “rainbow passage,” a paragraph read by test subjects as one of the exercises. Golshahi et al. developed five headforms—with surfaces of different materials—based on the anthropometric dimensions of a solitary female test subject. None achieved N95 FFs comparable to a good fit of the subject.<sup>[49]</sup>

To expand the information base and improve the protective capability of respirators—immediately against airborne transmission of influenza infections, ultimately in all contexts of airborne pathogens and, by obvious extension, to all particulate respiratory hazards—the Biomedical Research and Development Authority (BARDA) of the U.S. Department of Health and Human Services sponsored a program of basic investigations of aerosol–filter interactions by the Air Force Research Laboratory (AFRL). This effort included a systematic study comparing filtration efficiency of inert and pathogenic microbiological aerosols, which validated the common perception that both pathogenic and inert particles penetrate similarly.<sup>[50]</sup> The next step forward in this research is the design and construction of an articulated headform whose facial features are fabricated from a silicone that simulates human facial tissue and whose facial dimensions represent those identified by the NIOSH National Personal Protective Technology Laboratory as representative of the U.S. workforce.<sup>[51]</sup> This report describes the design, construction and initial testing of a static headform that is dimensioned to match the medium headform identified by NIOSH and includes these features, and the subsequent design and construction of an articulated headform that is able to reproduce human facial movements specified for fit testing, including those caused by reading the “rainbow passage.”

### 3. STATIC HEADFORM

#### 3.1. Headform Design Specifications

The static headform is of the medium size identified in the NIOSH “Principal Component Analysis (PCA) panel.”<sup>[51]</sup> The PCA panel was created using data from a large-scale anthropometric survey of U.S. workers conducted in 2003.<sup>[52]</sup> The PCA panel divides the user population into five face-size categories (small, medium, large, long/narrow, and short/wide). The PCA panel was developed using the first two principal components obtained from a set of 10 facial dimensions (age and race adjusted). These 10 dimensions are associated with respirator fit and leakage and can predict the remaining facial dimensions well. Respirators designed to fit the PCA panel are expected to accommodate more than 95% of the current U.S. civilian workers.<sup>[51]</sup>

#### 3.2. Headform Construction and Skin Covering

##### 3.2.1. Background

Human faces are both supple and conformable.<sup>[48,53]</sup> To achieve an adequate correlation in fit factor, the skin of a headform must conform to the respirator to obtain a seal comparable to that on a human face. A problem common to existing test headforms is the use of solid elastomers,<sup>[48]</sup> which are not as compliant and conformable as a human face, to simulate facial living soft tissues.<sup>[54]</sup> Human faces comprise mostly fluids, which deform under stress in ways that solid elastomer molecules cannot.<sup>[53]</sup> As no material existed with these properties, a conformable, supple “skin” was needed to cover a headform that can simulate respirator fit on human subjects.

Hanson Frubber™, a fluid-filled cellular matrix of elastomer, much more closely matches the physics of human facial living soft tissues than do previous elastomers.<sup>[53]</sup> Frubber™ compresses, elongates and otherwise deforms in ways that more accurately simulate human skin.<sup>[54]</sup> Originally developed to provide social robots with lifelike expressions to study human–robot interactions, Frubber™ was inspired by the physics of human soft tissues, in particular the role of surfactants in cell wall formation.<sup>[55]</sup> The resulting material weighs less, achieves better aesthetic reproduction of human facial expressions, and decreases the power consumed in actuation, which is important for bipedal mobility. The resulting robots display extremely humanlike emotions in numerous robotic applications, including the Diego-San robot (Figure 1), an ongoing project funded by the National Science Foundation (NSF) at the University of California San Diego Machine Perception Lab, Hanson Robotics and Kokoro Company, Ltd.<sup>[56]</sup>

The special properties of Frubber™ are achieved by a hybrid set of techniques including lipid bilayers at the nano scale and designed pore geometries for enhanced strength, supple flexibility, and elasticity.<sup>[55]</sup> These techniques may be tuned and combined to simulate a variety of properties of living soft tissue. The Frubber™ used in the headforms is made from polydimethylsiloxane (PDMS), cured with a platinum catalyst to promote stability and longevity. It is made porous by two major techniques: first, macropores are generated by creating a sacrificial matrix of soluble material, which is removed after the silicone sets, to leave a porous network. Next, a surfactant–oil–water mixture is used to facilitate the formation of 4–40 nm vesicles in the silicone elastomer.<sup>[54]</sup> This surfactant emulsion allows the geometry of the sacrificial matrix to migrate through the silicone material into a contiguous matrix, to achieve a geometry of pores tuned for the desirable mechanical properties of strength and elongation.

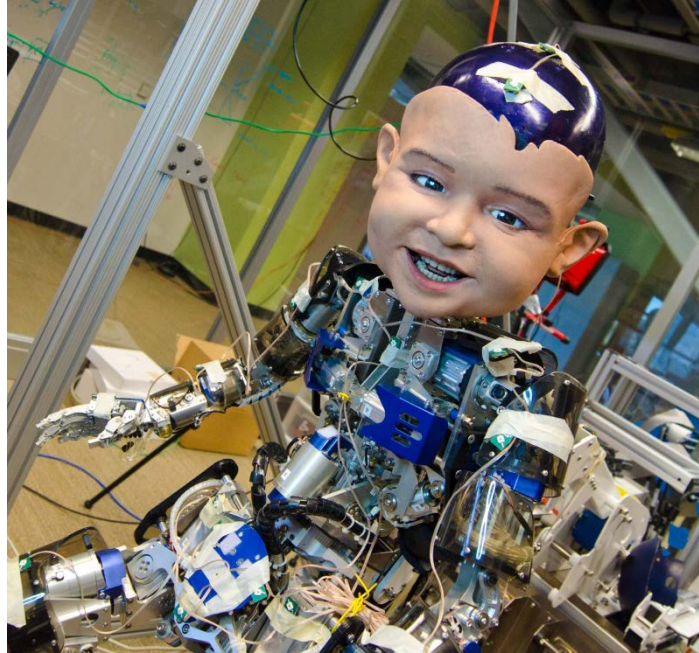


**Figure 1. 2010 Embodiment of Diego-San Robot, Which Uses Frubber™ to Create Humanlike Facial Expressions in a Mobile Robot Platform to Study Human–robot Interactions**

Additionally, the resulting reverse micelles serve as molecular-scale rip-stops, to deflect stress concentration when a tear happens due to molecular defects in the silicone material.<sup>[55]</sup> This results in a stronger, more supple silicone material with greater elongation.<sup>[55]</sup> Several special characteristics make Frubber™ a good synthetic skin for the application of simulating human faces in respirator fit testing. First, the softness of the material is comparable to that of human facial soft tissues,<sup>[55]</sup> as is the force required to elongate the material.<sup>[54]</sup> Second, because Frubber™ is a porous material, it is able to compress locally, in the manner of the fluid-filled cellular material of the human face, forming natural creases and folds, Third, the material is especially strong due to the molecular ripstop effect mentioned above.

The first 0.5 mm of the surface of Frubber™ is non-porous (or effectively so), and therefore has Poisson's ratio near 0.5. The next 1.0 mm of “tissue” (from 0.5 mm to 1.5 mm) has minimal porosity, and Poisson's ratio is estimated at 0.48. Porosity increases with distance from the surface. A macromolecular reverse-micelle technique is used to generate 4- to 40-nm pores (vesicles) filled with water and silicone oil. These reverse micelles are distributed throughout the Frubber™ and serve as nanoscale ripstops, functionally strengthening the base material.

To match the properties of the headform used in the described experiments to the human face, we developed a custom variation on the surfactant to tune the Frubber™ formula. By tuning the proportions of oil, water, surfactant, dextrose, sodium chloride and PDMS, we create a chaotic condition that gives rise to self-assembling complex porous structures, which can be controlled to tune the hardness, Young's modulus and Poisson's ratio to match those properties of skin. The progression in Figure 2 shows the increased complexity from the conventionally prepared leftmost sample, to the custom-tuned formulation of the rightmost sample, which exhibits

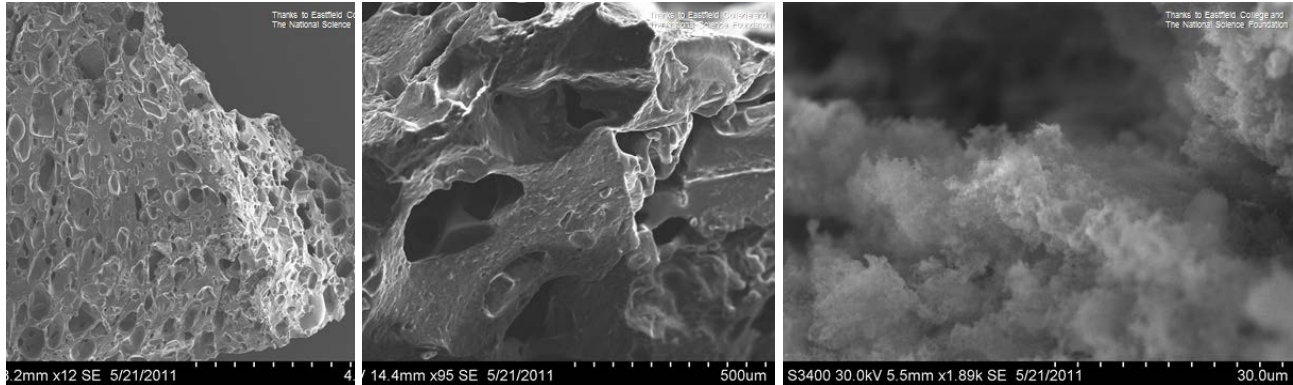


**Figure 2. Scanning Electron Micrographs, Showing Increased Hierarchical Porosity in the Rightmost Sample (Courtesy of NSF funding and Richland College in Dallas)**

hierarchical porosity down to submicron scale. These scanning electron micrographs, courtesy of NSF funding and Richland College in Dallas, helped to validate some of the exotic properties of Frubber™ that result in more-lifelike facial deformations and expressions.

### 3.2.2. Materials and Methods

The headform was created in several stages. First, an acrylonitrile–butadiene–styrene (ABS) plastic model was made of the medium-sized NIOSH digital headform (Figure 3) described by Zhuang et al.<sup>[57]</sup> To achieve the design task of generating a skin with correct thickness, Hanson Robotics conducted the physical fabrication, mold creation, mechanical design and fabrication of the static headform.



**Figure 3. NIOSH Standard Medium Headform**

At the outset it was recognized that, for the headform to accurately simulate a human face in fit testing, it would be necessary to add in characteristic, properties and details of the human face, such as skin texture, mouth form, lip physiology, nose detail and neck anatomy, which are absent from the NIOSH headforms. So for the described experiments, Hanson Robotics created a mold (a negative tool) of the ABS plastic model of the headform, which was cast as a replica in clay. Then additional details were introduced into the surface of the clay form by sculpting anatomically accurate skin texture, nose forms, and lip and mouth features (Figure 4).



**Figure 4. NIOSH Medium Headform with Additional Details**

The new designs resulted in revisions to original quotes for the computer numerical control–computer-aided manufacturing (CNC-CAM) execution of the digital design of the tooling. At this point, Hanson Robotics created a new mold of this more refined headform (Figure 5).

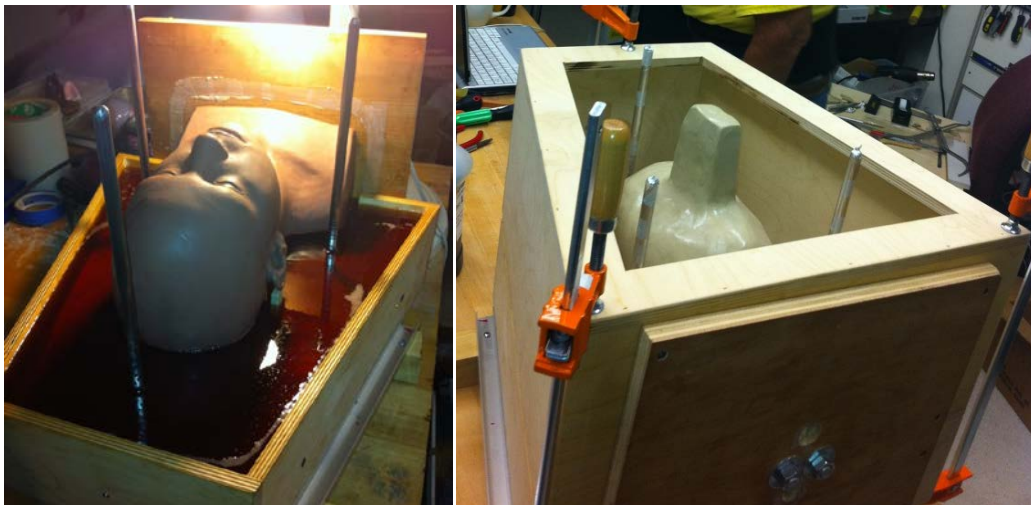


**Figure 5. Mold of the Detailed NIOSH Medium Headform**

The facial thickness values used in building the advanced headform were based on a large-scale study of facial tissue thickness conducted recently by De Greef et al., in which an ultrasound-based measuring system was used to determine facial thickness.<sup>[58]</sup> The data collected in De Greef’s study were tabulated according to gender, age, body-mass index (BMI), and anatomical location (face landmark). The values specified for the advanced headform are for male Caucasians 18–29 years old with  $20 \leq \text{BMI} \leq 25$  (Figure 6).

Hanson Robotics created a digital 3D representation of this map as a design study (Figure 7), from which a strategy for physical implementation was derived, wherein greater anatomical accuracy would be achieved, by physically sculpting this skull form within the mold.

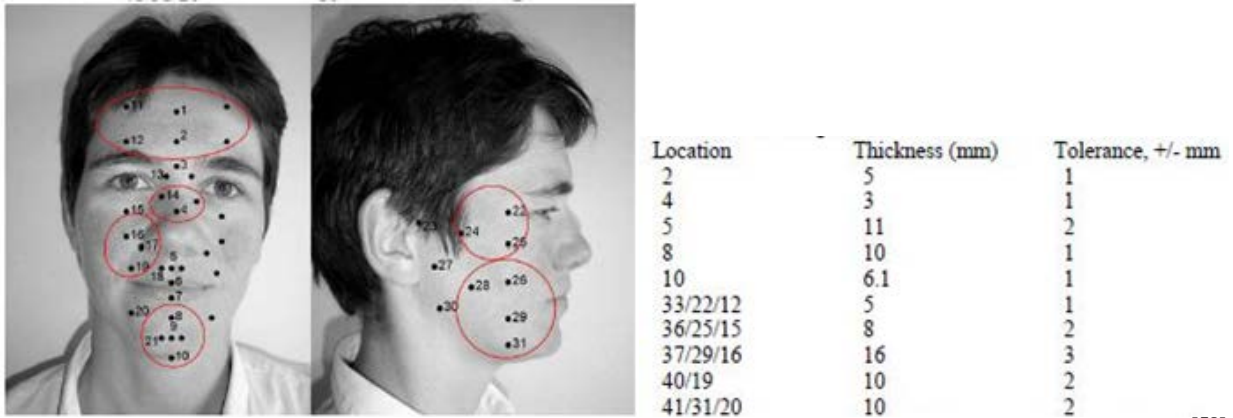


**Figure 6. Locations of Landmarks of Variable Thicknesses of Human Facial Soft Tissue<sup>[58]</sup>**

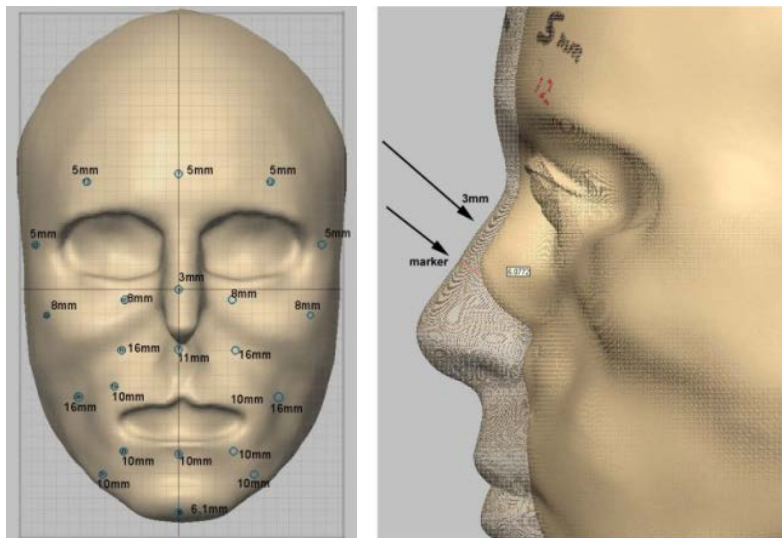


**Figure 7. 3D Design Study of Facial Landmark Thickness**

To generate the tissue thicknesses of the “skin” surface within the mold of the NIOSH medium headform and cast an anatomically accurate skull form, Hanson Robotics carefully measured spacers/jigs pinned within the cavity of the mold, approximately normal to the surface, as shown in Figure 8. This process is analogous to forensic facial reconstruction, with the exception that the techniques here were applied in reverse, to achieve a skull from a facial form rather than a face form from a skull.

When the jigs were in place, clay was applied into the face form and sculpted among the spacers, as an iterative, spreading process in which repeated measurements and progressive sculpting of more locations was employed to attain anatomical accuracy. Clays of different colors represent differing regimes of thickness in the facial tissues, as illustrated in Figure 9.



**Figure 8. Face Mold Negative Form with Tissue Thickness Markers Emplaced**

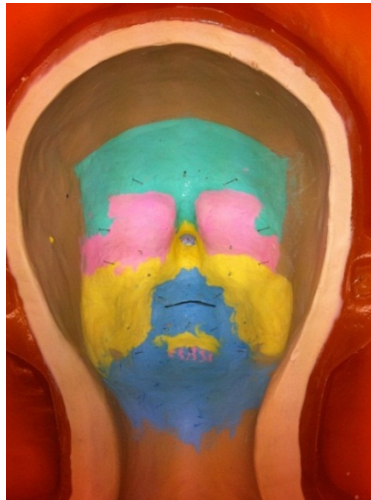


**Figure 9. Reverse Forensic Facial Reconstruction Used to Generate Anatomically Accurate Skull Form**

Dimensions of this skull form were validated against anatomical models of the skull, and tissue thicknesses were tested using depth gauges throughout the clay form. Once this sculpture was completed, a rigid urethane plastic mixture was poured into the negative form of the clay to produce a positive core of the tool, with registration tabs that connect to the tool of the face form, to ensure that the two precisely register during the Frubber™ casting process. This plastic skull form was then checked for accuracy, and features were added for later registering the cast skin on the skull form. The skull form was then laser scanned to provide a 3D model for digital design verification (Figure 10). After this, a tool was made of the skull and a reproduction of the skull was made in rigid urethane plastic (Task 9<sup>[59]</sup>, Smooth-on, Inc., Easton, PA), with an integrated PVC pipe (1-in ID) breathing channel cast directly into the skull, leading from the mouth region to the base of the neck.

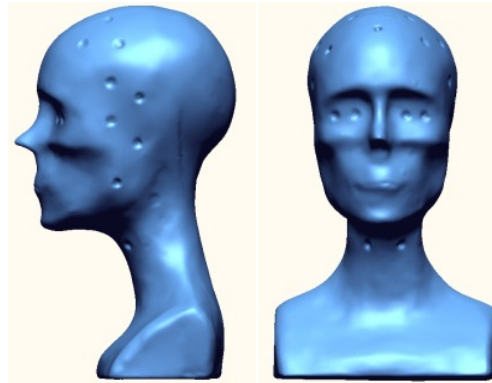


**Figure 10. Laser Scan of the Skull, Showing Registration Features**

Next, the skull form was installed in the face mold with the locating pins and a Frubber™ “skin” was cast into the mold, filling the space between the skull form and mold, and thereby reproducing anatomically accurate tissue thicknesses. During this process a patch of reinforcing cloth was added to the “bridge” of the nose—the region of the procerus muscle, at the top of the nose. The skin was then glued to the surface of the cast skull form using Platsil Gel-10 silicone adhesive (Polytek, Easton, PA). The skin was rigorously measured with a lance to validate the accuracy of the tissue thicknesses. The resulting punctures in the skin were sealed with more Platsil Gel-10 to achieve a watertight seal of the skin for respirator testing. The completed headform was mounted on a portable acrylic base and prepared for use in the laboratory (Figure 11).



**Figure 11. Static Headform with Anatomically Accurate Facial “Skin” Thicknesses**

Completing the assembly, we sealed the 2-in section of PVC pipe projecting out the bottom of the base (for attaching a breathing machine to draw air [and allow collection of samples without disturbing the respirator being tested]) through the tube to be watertight. The entire headform was checked to verify the watertight seal and material properties of the skin prior to its shipment to AFRL.

## 4. ARTICULATED HEADFORM

### 4.1. Design Changes and Component Assembly

#### 4.1.1. Adjustments after Initial Headform Testing

Feedback from NIOSH about the static headform indicated that the temples and back of the head were too small (violet and dark blue areas in Figure 12), which resulted from deformation of the surface during the assembly process. We devised jigs to control the surface form during assembly and to verify dimensions prior to shipment.

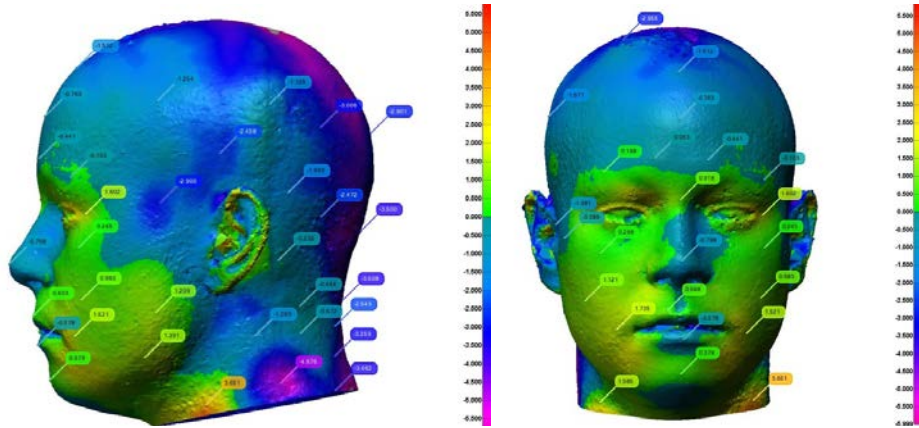


Figure 12. NIOSH Surface Form Evaluation, Correlated with the NIOSH Medium File

#### 4.1.2. Evolution of Skull Design

Mean time between failure (MTBF) testing and analysis of two brushless servo models, Futaba BLS 0153 and BLS 0157 (Figure 13), showed them to be 100% reliable for an extended testing period, consistent with the manufacturer's MTBF statistics. As they are brushless, we expected them to perform as the manufacturers' data claim and last considerably longer than the motors originally specified in our proposal, so we were confident that this was a design improvement.



Figure 13. Brushless Servo Selected for Implementation

The new servo is physically larger than the original, so this substitution drove a redesign (Figure 14, right) of the original articulated skull form (Figure 14, left) to accommodate the dimensional change. We proceeded cautiously with the mechanical design, pending the possibility of changes to the skull-form required as a result of NIOSH and AFRL testing of the first static headform. To allow for possible changes to skull form that might appear after testing of the static headform, mechanical design work for several weeks was done within a conservatively small envelope, with allowance for a 5-mm margin of error.

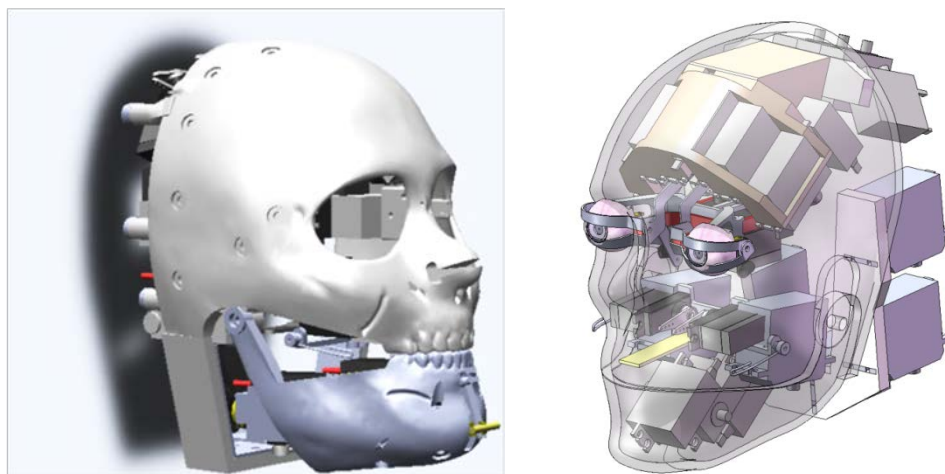


**Figure 14. Skull Forms, As Originally Proposed (left) and Revised to Emplace the Brushless Servos (right)**

To accommodate the possibility of building the four additional NIOSH headforms we continued the refinement of mechanical design of the articulated headform in such a way that the design was flexible to allow for changes to proportions in the skull if necessary (see Figure 15). In the process of this design revision, we fitted all the degrees of freedom within the mechanical envelope, and accommodated the flexible breathing tube and passageway.



**Figure 15. Second Redesign of Articulated Skull Form**

We began to modify the skull form to include such features as teeth, and the registration system to control the positioning of the Frubber™ on the skull without compressing the surface form of the Frubber™. Responding to a request from the AFRL program manager we modified the skull design to allow for easy removal of the back of the skull for maintenance, and a gasket to provide a watertight seal to isolate the internal mechanics and electronics from exposure to salts and water during aerosol challenges.

Good progress was also made on the custom anchor design for the articulated headform [to realize accurate humanlike expressions]. Fabrication of internal mechanical systems was started in February 2012, including machining aluminum and steel parts, and rapid prototyping of ABS plastic components. As these parts were completed, mechanical assembly of the internal mechanics was begun. A headform assembled during March 2012 was partially successful in testing but was dismantled and the components salvaged. Progress through April on the skull design can be seen in Figure 16, which shows teeth and the removable back of the head. Figure 17 illustrates the custom anchor design (on a static skull form), which provide attachments to servos to provide movement and expression in the lower face.

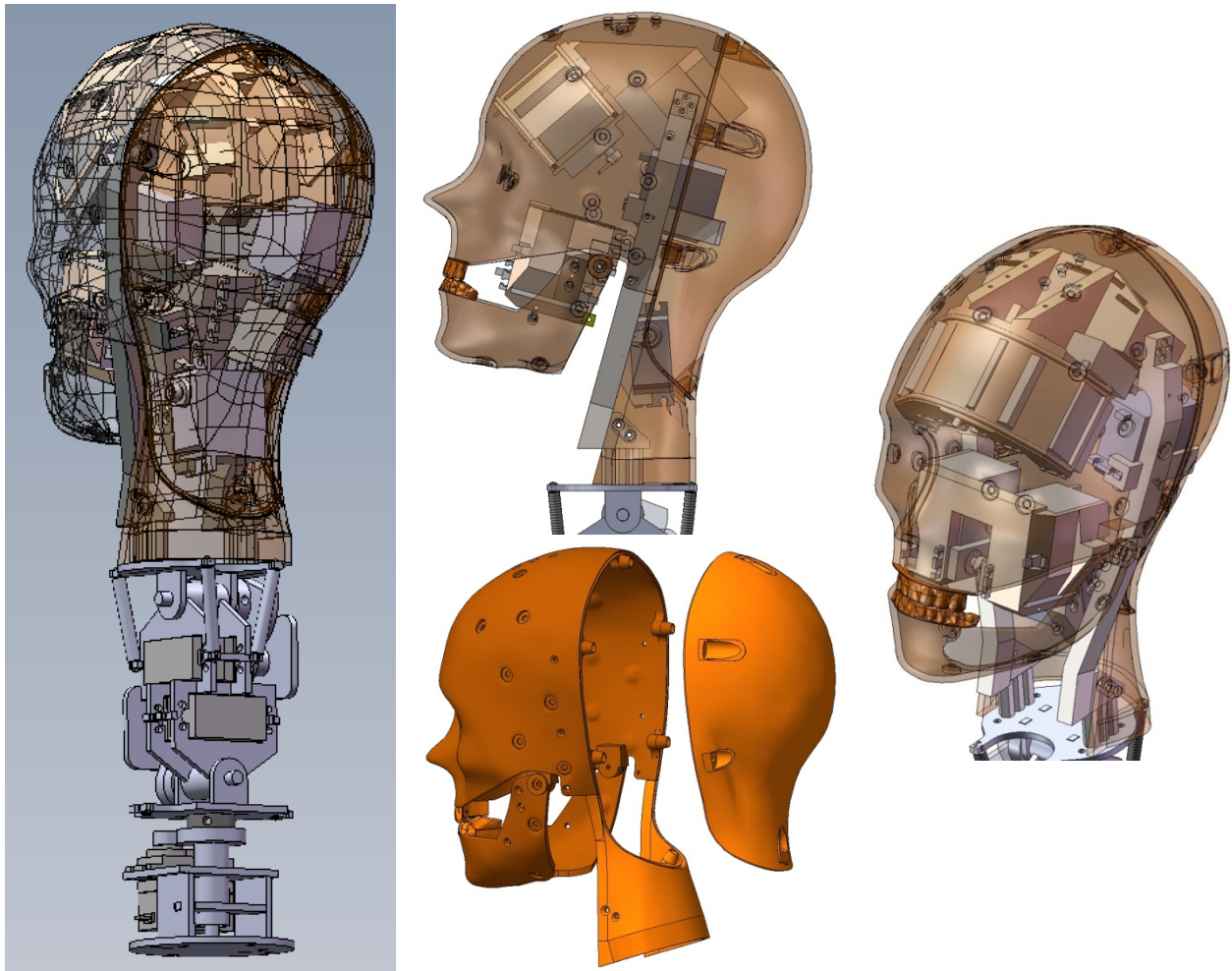


**Figure 16. Mechanical Designs, Showing Gasket-sealed Maintenance Access Panel, Neck Integration and Initial Servo Configuration**



**Figure 17. Expression Anchor Implementations**

Several mechanical problems surfaced during the evolution of the articulated skull. Penetration of the cables seen in Figure 17 through the oral cavity interfered with the breathing tube, which occupied the same space; conversion to (larger) coreless motors to improve reliability exacerbated this problem. We sacrificed anatomical accuracy to solve this problem by routing the air upward and over the top of the head. When we cast the skin with anchors to connect to the cables shown in Figure 17 the new formulation swelled by ~5 percent. Iterative washing and baking of the skin eventually achieved the proper dimensions, but attachment to the skull and testing showed the mechanical properties to be unsatisfactory. A series of experiments adjusting the quantities of glucose, water and silicone oil in the PDMS formulation identified a composition that retained dimensional tolerances and displayed physical properties within the standards set in the contract. Figure 18 shows the articulated skull form and the articulating mechanism at this stage, and Figure 19 compares appearances of the original and improved Frubber™ skins.

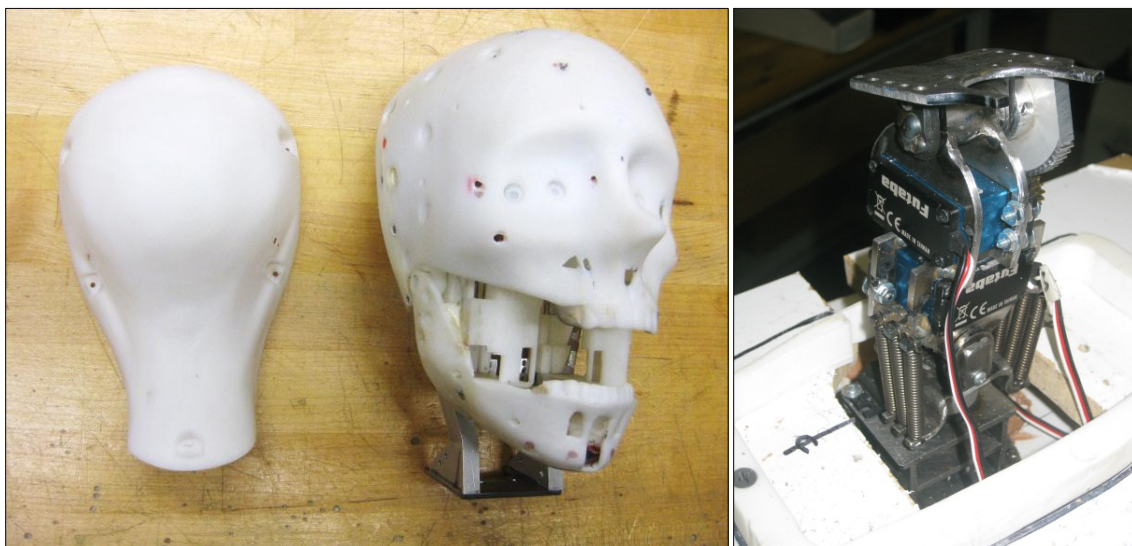
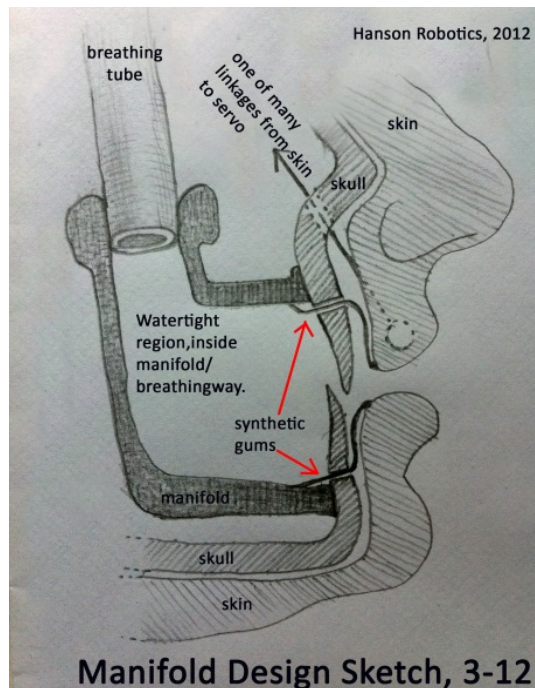


**Figure 18. Articulated Skull Form (left) and Articulated Support (Neck)(right)**



**Figure 19. Initial (left) and Improved Articulated Skin Implementations**

From March to June 2012 a series of prototypes were assembled, tested, dismantled and recycled in the course of sealing the airway from the electronics, isolating the airway from interference with cables to anchors, and achieving a full range of motion of the mouth, jaw and emotional muscles—all formidable challenges. We were able to configure the oral cavity as a compliant manifold, custom crafted to contour to the skin and skull, and flexible enough to provide the complete range of mouth and jaw motions and lower facial expressions (Figure 20). As part of this step we developed synthetic gums as a platinum-cured silicone calendared to 2-mm thickness over an Elastane–nylon fabric (Figure 21). This produced a strong, watertight membrane



**Manifold Design Sketch, 3-12**

**Figure 20. Design Sketch of Oral Cavity Manifold**



**Figure 21. Oral Cavity Manifold; Side (left) and Front Views (center) Closed, and Front View Open (right)**

that exhibited excellent flexibility and that extended from the manifold to adhere to the inside of the skin around the lips. Individual teeth were included in the design, to screw through the gums and into the skull, and to seat in watertight gaskets to protect the screws from corrosion.

Realization of the flexible breathing tube was accomplished as shown in Figure 22. Carrying the flexible tube over the top of the head and down the back of the skull allowed adequate clearances to fit mechanical components and achieve the necessary ranges of motion of the jaw. The manifold was cast to formfit the breathing tube, which we increased to 1-in inside diameter (ID), with an airtight/watertight seal low in the area of the jaw (Figure 23). The top view illustrated in Figure 24 clearly shows the locations under the manifold of the mechanical elements driving the lower lip, which require that the breathing tube pass elsewhere.

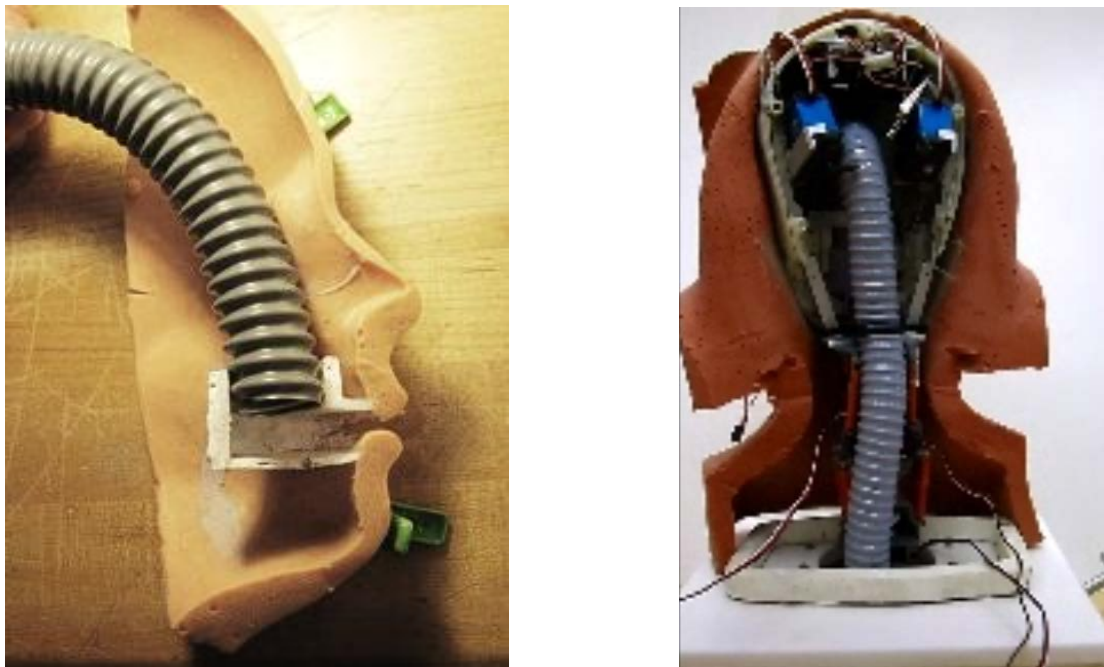


**Figure 22. Side (left) and Rear Views (right) of Trajectory of Breathing Tube**

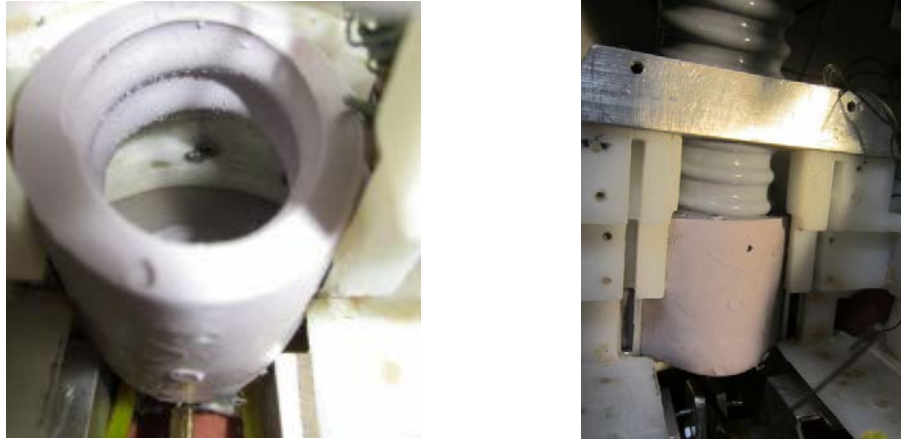


**Figure 23. Manifold–Breathing Tube Joint; Top View of Connection (left) and Rear View Showing Breathing Tube Installed**

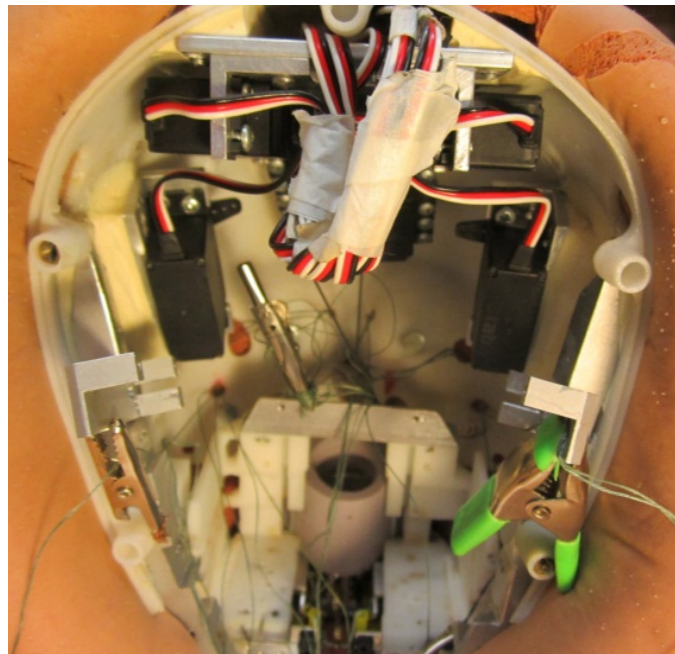


**Figure 24. Rear View of Skull Form Showing Components Surrounding Manifold–Breathing Tube Joint**

We completed the registration systems to removably anchor the skin to the skull, by bolting the skin to the eye sockets and registering snaps around the perimeter of the facial actions. We also changed the mechanics of the zygomaticus muscles and the nasalis and orbicularis oris muscles, to achieve more natural actions in these areas and still accommodate the breathing tube, and we reconstructed the jaw actuation mechanics to accommodate the manifold while still effectuating the full range of “natural” mouth actions. It was necessary also to redesign the neck (Figure 25) to fit into a smaller envelope, to accommodate the increased size of the breathing tube (1 in ID instead of the original  $\frac{3}{4}$  in), without distorting the neck skin.



**Figure 25. Original (left) and Redesigned Neck Structures (center, right)**

Adjustments to the design of the mechanical systems inside the headform were necessary to allow the breathing tube and manifold to function properly and allow for ease of maintenance. It was also necessary that the system continue to achieve the specified simulated muscle mechanics with the larger servomotors. We hand-crafted the solutions and, in the process, we adjusted the positions of the degrees of freedom within the mechanical envelope and accommodated the flexible breathing tube and passageway. We drew these design changes in our CAD SolidWorks models, to accelerate the reproduction of these design elements for the second articulated headform.

Heat from powered components is removed by circulating air through the interior space. For this headform an aquarium pump was located in the base to draw air through the headform and exhaust it underneath. To put the interior volume at positive pressure to the aerosol stream in the breathing passage, the pump will be installed to push rather than pull air in the second headform.

#### **4.1.3. Software and Integration**

We enhanced our existing software and electronics systems in several ways. Sensing of motor operation was improved, and automated user notification of motor errors was incorporated as a feature. Data logging was added, and a user manual (Appendix) prepared. As a matter of practicality, to limit cost and simplify both production and maintenance, we were advised to replace the teeth with a simple ridge. Final assembly of the first articulated headform was completed in August 2012. Several weeks of tests established that it performed to specifications and it was shipped to AFRL during September. Opportunities for improvements noted during final assembly and testing will be incorporated in the construction and assembly of the second article.

## 5. DISCUSSION

### 5.1. Static Headform

Except for slight deformations of the top of the head, the static headform accurately reproduced the dimensions of the NIOSH medium headform. The appearance and texture were lifelike—if perhaps a bit cadaverous—and fit testing with a panel of seven respirators known to achieve FFs > 100 after proper donning on the majority of wearers revealed average FFs close to 200 after proper donning and >200 when a pretest using a Portacount system eliminated the less-effective donnings (Figure 26).<sup>[61]</sup>

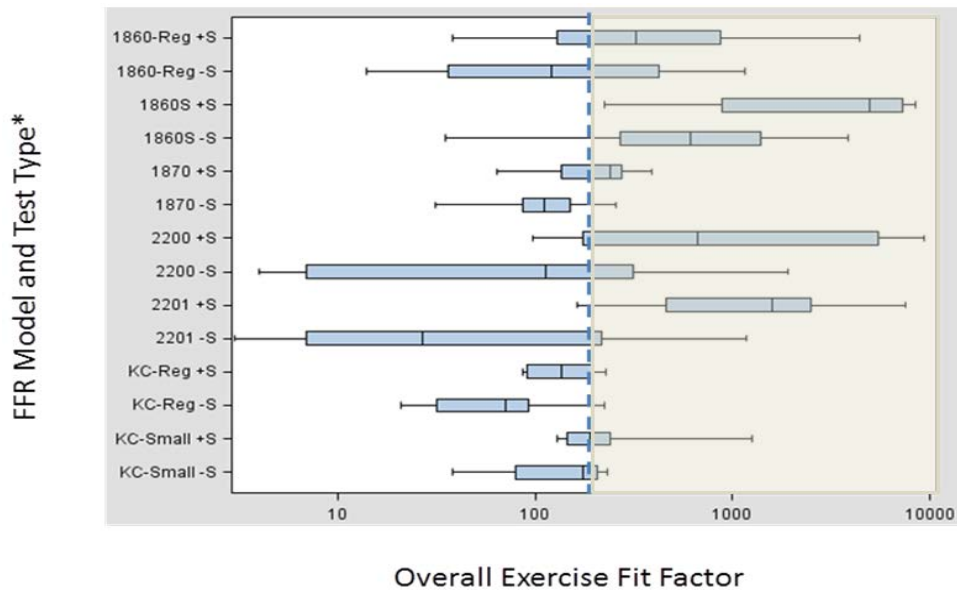


**Figure 26. Distribution of Geometric Mean Fit Factors (n = 112 Data Points)<sup>[61]</sup>**

The conditions of the test excluded the movement included in full respirator fit testing, so the higher FFs on the headform are certainly due at least in part to the simplification of the test. That almost a third of donnings gave fit factors < 100 provides clear evidence that the static headform is a “typical face,” and likely to prove to be suitable for the intended purpose of limiting human involvement in routine respirator testing and enabling exercises in which fit/leak/penetration testing respirators involves challenges by hazardous or pathogenic particles (or vapors and gases).

### 5.2. Articulated Headform

The revolutionary nature of the articulated headform is evident from a glance at the challenges that surfaced as the design evolved during the course of the development, causing it to escalate from a daunting challenge to an almost Sisyphean task. The requirement to match skin thickness of the headform to data from ultrasound studies was largely attended to during the development and construction of the static headform, but the texture of the Frubber™ composition used in the static headform did not hold up during casting onto anchor points and it was necessary to explore

a series of reformulations to achieve a composition that both retained its dimensions and deformed realistically when driven by the servos.

Replacement of the brushed motors originally proposed improved the reliability and service lifetime of the articulated headform, but their increased footprint was one of several factors that required a series of iterative design modifications of and primarily inside the skull form. The dimension of the breathing tube was increased by ¼ in, and the network of hardware driving motion in and of the jaw and lips so filled the lower jaw area that it was necessary to route the airflow up and over the top of the components in the skull form to exit at the base of the neck.

The single greatest challenge—which was not explicit at the start of the project—was isolating the mechanical components and associated electronics from the airflow, which will typically contain water and salts. After a series of dead ends and brainstorming sessions we devised a flexible plenum to occupy the “oral cavity” of the headform, which sealed to the lips of the face under artificial gums that were designed to accept and seal off threaded teeth. Air exits the top of the plenum through a threaded fitting that engages the breathing tube, and the breathing tube projects through a second seal at the base of the neck, which isolates the functional components. Access for maintenance was provided by making the back of the head removable and fitting the mating surfaces with a flexible gasket to provide an air- and water-tight seal.

The deformations mentioned in 5.1 were eliminated by a combination of using a jig for assembly and measuring dimensions as a pretest for acceptance, and installation of fixed attachment points at several locations near the “eyes” and edges of the skull form.

### **5.3. General**

At the conclusion of the contract performance period only one static and one articulated headform have been delivered, and test data exist for only the static article. Construction of the second articles is well underway.

The initial results are gratifying in the extreme but the acid test of the headform is scheduled at NIOSH—a statistical exercise in which FFs measured for both respirators from the group tested and two respirators that have a less-auspicious history of fit testing, to establish the representativeness (or lack thereof) of the articulated headform as a respirator fit test panelist. As of this writing the protocol has received full approval and most of the panel of 10 human testers has been recruited. Onsite integration of the software packages to reproduce the complete fit protocol is nearing completion. A successful conclusion of that exercise will qualify the headform to undertake development and, one hopes, eventual establishment of a certification protocol for FFRs that measures net protection—penetration of the medium plus inward leakage through seals and breaches—to replace the 42 CFR 84 standard, which measures only fractional penetration of the filter medium. Hanson Robotics plans to develop a commercial market for the headforms in support of the use of the same method for FFR development and quality control testing, and for certification of new FFRs. The initial target is to support an N95 certification protocol that aligns with the OSHA standard.

Concurrent development at AFRL of an aerosol exposure chamber and a versatile breathing simulator able to operate at peak rates of 10–360 L/min is expected to couple with the second

headform to provide an integrated system—a robotic test subject that can be exposed to challenges that no human-use panel would condone, that does not fatigue, call in sick or goldbrick, and that can be challenged to study protectivity of IRP devices worn under conditions of extreme physical duress. Extension of this type of testing we also see as a potential market to both military labs and to developers and suppliers of IRP gear.

#### **5.4. Conclusions**

Despite misadventures of cost and schedule this project has been an eminently successful technical venture. The technical goals met to date have clearly met their targets, and initial indications suggest that the remaining goals—most importantly the statistical correlation with the NIOSH wearer panel—will also be realized. The Air Force is receiving a tool for respirator fit testing that is unique in two contexts: first, the headform—in combination with the breathing simulator developed by AFRL— is equivalent to a human for respirator leak testing; and second, the headform offers the advantages of being able to perform 24/7 and to undergo testing with hazardous challenges (e.g., pathogens, toxic industrial chemicals, chemical/biological warfare agents compatible with silicones) to which human volunteers could ethically not be exposed (i.e., human use panels would never approve). It is our confident expectation that the new headforms herald a new generation of improved respiratory protective gear and a clear understanding of the protectivity afforded by and performance limits of fielded and candidate IRP gear in military, medical, industrial and civilian applications. Hanson’s goal of marketing a commercial product will support all of the above.

## 6. REFERENCES

1. Barbalace, R.C., *A Brief History of Asbestos Use and Associated Health Risks*  
<http://environmentalchemistry.com/yogi/environmental/asbestoshistory2004.html>
2. OSHA, *Industrial Hygiene*[:] *Extracts*, <http://actrav.itcilo.org/actrav-english/telearn/osh/hazard/hyg.htm>
3. John Bostock, “Chapter 40, The Various Kinds of Minium. The Use Made of it in Painting,” in *Pliny the Elder, The Natural History, Book XXXIII. The Natural History of Metals*.  
<http://www.perseus.tufts.edu/hopper/text?doc=Perseus:abo:phi,0978,001:33#note-link356>
4. Davis, T.L., and J.R. Ware, Early Chinese Military Pyrotechnics, *J. Chem. Ed.*, **24**, 522–537 (1947).
5. Smart, J. K. History of chemical and biological warfare: An American perspective. In *Textbook of Military Medicine, Part I. Warfare, Weaponry, and the Casualty. Medical Aspects of Chemical and Biological Warfare* (pp. 9–86). Washington, DC: Office of the Surgeon General, Walter Reed Army Medical Center. 1997.
6. McCurdy, E. (Ed.). *The notebooks of Leonardo da Vinci* (Vol. 2). London, England: Jonathan Cape. 1977
7. Hoover, H.C., and L.H. Hoover, *Georgius Agricola*[:] *De Re Metallica*, The Mining Magazine, Salisbury House, London, 1912. p. 215.
8. Dictionary Definition: Respirator, <http://respirator.askdefine.com/>; Gupta, R., *Respirators and Face Masks*, <http://www.buzzle.com/articles/respirators-and-face-masks.html>
9. Haslett, L.P., *Inhaler or Lung-Protector*, U.S. Patent 6,529, 12 June 1849.
10. Hurd, H.R., *Improvement in Inhaler and Respirator*, U.S. Patent 218,976, 26 August 1879.
11. Miles, W.D., “[The velvet-lined gas mask of John Stenhouse.](#)” *Armed Forces Chemical Journal*, **12**(3), 24–25 (1958).
12. Stenhouse, J., “[On the economical applications of Charcoal to Sanitary purposes \[2 March 1855\].](#)” *Notices of the Proceedings at the Meetings of the Members of the Royal Institution of Great Britain with Abstracts of the Discourses Delivered at the Evening Meetings*, vol. 2, William Clowes and Sons, London, 1858. pp. 53–55.
13. Tyndall, J., On Dust and Disease, Chapter 11, *Fragments of Science for Unscientific People: A Series of Detached Essays, Lectures, and Reviews*, Appleton, New York, 1871. pp. 316–317.
14. Tyndall, J., On some recent Experiments with a Fireman’s Respirator, *Proceedings of the Royal Society of London*, **22** (148–155), 359–361 (1874).
15. Second Battle of Ypres, [http://en.wikipedia.org/wiki/Second\\_Battle\\_of\\_Ypres](http://en.wikipedia.org/wiki/Second_Battle_of_Ypres) includes many relevant sources.
16. Respirator, <http://en.wikipedia.org/wiki/Respirator>
17. *Nuclear Air Cleaning Handbook*, DOE-HDBK-1169-2003, pp. 1-1–1-3.
18. Gilbert, H.; Palmer, J.H. 1961. *Inspection, Storage, Handling and Installation of High-Efficiency Particulate Air Filter Units*, USAEC Report TID-7023.
19. Davies, C.N. *Air Filtration*, Academic Press, London, 1973.
20. *ibid.*, p. 142.

21. Freundlich, H., *Colloid and Capillary Chemistry*, (translated by Hatfield, H.S.), Methuen, London, 1926. p. 785.
22. Kaufman, A., Die Faserstoffe für Atemschutzfilter[:] Wirkungsweise und Verbesserungsmöglichkeiten, *Zeitschrift des Vereines deutscher Ingenieure*, **80**(20): 593–600 (1936).
23. Lushkinov, A., “Igor Vasilievich Petryanov–Sokolov (1907–1996),” *J. Aerosol Sci.*, **28**(4): 545–546. 1997.
24. Herris, W.P. “How Regulation and Innovation Have Shaped Respiratory Protection,” [http://ehstoday.com/ppe/respirators/regulation\\_innovation\\_shaped](http://ehstoday.com/ppe/respirators/regulation_innovation_shaped)
25. *NIOSH Guide to the Selection and Use of Particulate Respirators Certified under 42 CFR 84*. DHHS (NIOSH) Publication Number 96-101. <http://www.cdc.gov/niosh/docs/96-101/>; NIOSH, *Respiratory Protective Devices. 42 Code of Federal Regulations Section 84*, US Government Printing Office, Office of the Federal Register: Washington, DC, 1995.
26. European Committee on Standardization, EN 143:2000 *Respiratory Protective Devices: Particle Filters—Requirements, Testing, Marketing*. <http://esearch.cen.eu/esearch/Details.aspx?id=7052213>.
27. European Committee on Standardization, EN 149:2001+A1:2009 *Respiratory Protective Devices: Filtering Half Masks to Protect Against Particles—Requirements, Testing, Marketing*. <http://esearch.cen.eu/esearch/Details.aspx?id=7086991>.
28. Occupational Safety and Health Administration (OSHA), *Respiratory Protection: Final Rule*, 1998, US Government Printing Office, Office of the Federal Register: Washington, DC.; OSHA, *Occupational Safety and Health Standards, I, Personal Protective Equipment, Respiratory Protection*, [http://www.osha.gov/pls/oshaweb/owadisp.show\\_document?p\\_table=STANDARDS&p\\_id=12716](http://www.osha.gov/pls/oshaweb/owadisp.show_document?p_table=STANDARDS&p_id=12716).
29. *OSHA Technical Manual (OTM)*, Section VIII: Chapter 2. [http://www.osha.gov/dts/osta/otm/otm\\_viii/otm\\_viii\\_2.html](http://www.osha.gov/dts/osta/otm/otm_viii/otm_viii_2.html).
31. Coffey, C.C., et al., Comparison of five methods for fit-testing N95 filtering-facepiece respirators. *Appl. Occup. Environ. Hyg.*, 2002. **17**(10): 723–730; Coffey, C.C., et al., Fitting characteristics of eighteen N95 filtering-facepiece respirators. *J. Occup. Environ. Hyg.*, 2004. **1**(4): 262–271.
32. Campbell, D.L., C.C. Coffey, and S.W. Lenhart, Respiratory protection as a function of respirator fitting characteristics and fit test accuracy. *Am. Ind. Hyg. Assoc. J.*, 2001. **62**(1): 36–44.
33. Coffey, C.C., D.L. Campbell, and Z. Zhuang, *Simulated workplace performance of N95 respirators*. *Am. Ind. Hyg. Assoc. J.*, 1999. **60**(5): 618–624.
34. Zhuang, Z., et al., Correlation between quantitative fit factors and workplace protection factors measured in actual workplace environments at a steel foundry. *Am. Ind. Hyg. Assoc. J.*, 2003. **64**(6): 730–738.
35. Han, D.H. and J. Lee, Evaluation of particulate filtering respirators using inward leakage (IL) or total inward leakage (TIL) Testing—Korean experience. *Ann. Occup. Hyg.*, 2005. **49**(7): 569–574.

36. Grinshpun, S.A., et al., Performance of an N95 filtering facepiece particulate respirator and a surgical mask during human breathing: two pathways for particle penetration. *J. Occup. Environ. Hyg.*, 2009. **6**(10): 593–603.
37. Clayton, M. and N. Vaughan, Fit for purpose? The role of fit testing in respiratory protection. *Ann. Occup. Hyg.*, 2005. **49**(7): 545–548.
38. Cooper, D.W., et al., Common materials for emergency respiratory protection: leakage tests with a manikin. *Am. Ind. Hyg. Assoc. J.*, 1983. **44**: 720–726.
39. Tuomi, T., Face seal leakage of half-masks and surgical masks. *Am. Ind. Hyg. Assoc. J.*, 1985. **46**(6): 308–312.
40. Cohen, K., *Report No. ARL-TR-2070. Relationship of Protective Mask Seal Pressure to Fit Factor and Head Harness Strap Stretch*. Report to Army Research Laboratory. 1999.
41. Vaughn, N., A. Tierney, and R. Brown, Penetration of 1.5–9.0  $\mu\text{m}$  diameter monodisperse particles through leaks into respirators. *Ann. Occup. Hyg.*, 1994. **38**(6): 879–893.
42. Hinds, W.C. and G. Kraske, Performance of dust respirators with facial seal leaks: I. Experimental. *Am. Indust. Hyg. Assoc. J.*, 1987. **48**(10): 836–841.
43. Rengasamy, S. and B.C. Eimer, Total Inward Leakage of Nanoparticles Through Filtering Facepiece Respirators. *Ann. Occup. Hyg.*, 2011. **55**(3): 253–263.
44. Chen, C.C. and K. Willeke, Characteristics of face seal leakage in filtering facepieces. *Am. Ind. Hyg. Assoc. J.*, 1992. **53**(9): 533–539.
45. Krishnan, U., et al., Variation in quantitative respirator fit factors due to fluctuations in leak size during fit testing. *Am. Ind. Hyg. Assoc. J.*, 1994. **55**(4): 309–314.
46. Janssen, L. and R. Weber, The effect of pressure drop on respirator face seal leakage. *J. Occup. Envi. Hyg.*, 2005. **2**(7): 335–340.
47. Janssen, L.L., T.J. Nelson, and K.T. Cuta, Workplace protection factors for an N95 filtering facepiece respirator. *J. Occup. Envi. Hyg.*, 2007. **4**(9): 698–707.
48. Richardson, A., A. Wang, and K. Hofacre, *Development of Skin-Like Material to Accommodate Respirator Sealing with Manikin Head Forms*, in Report to U.S. Army Edgewood Chemical Biological Center, 2007.
49. Golshahi, L., et al., A pilot study on the use of geometrically accurate face models to replicate ex vivo N95 mask fit. *Am. J. Infect. Control*, 2012. DOI:10.1016/j.ajic.2012.01.008
50. Wander, J. and B. Heimbuch, *Challenge of N95 and P100 Filtering Facepiece Respirators with Particle Containing Viable H1N1, NIOSH IAA # 09-42, CDC Agreement IAA #09FED905877*. Submitted to NIOSH/NPPTL, 2009.
51. Zhuang, Z.Q., B. Bradtmiller, and R.E. Shaffer, New respirator fit test panels representing the current US civilian work force. *J. Occup. Envi. Hyg.*, 2007. **4**(9): 647–659.
52. Zhuang, Z.Q. and B. Bradtmiller, Head-and-face anthropometric survey of US respirator users. *J. Occup. Envi. Hyg.*, 2005. **2**(11): 567–576.
53. Hanson, D. and S. Priya, *An Actuated Skin for Robotic Facial Expressions*, NSF Phase 1 Final Report. National Science Foundation STTR award, NSF 05-557, 2006–2007.
54. Hanson, D. and V. White, Converging the Capabilities of ElectroActive Polymer Artificial Muscles and the Requirements of Bio-inspired Robotics. *Proc. SPIE's Electroactive Polymer*

*Actuators and Devices Conf., 10th Smart Structures and Materials Symposium, San Diego, 2004.*

55. Hanson, D., et al., Enhancement of EAP Actuated Facial Expressions by Designed Chamber Geometry in Elastomers. *Proc. SPIE's Electroactive Polymer Actuators and Devices Conf., 10th Smart Structures and Materials Symposium, San Diego.* 2006.
56. Ruvolo, P., T. Wu, J.R. Movellan, *Studying Mother–Infant Interaction Using Motion Capture* [http://tdlc.ucsd.edu/research/posters/AHM\\_2011/paul\\_ruvulo.pdf](http://tdlc.ucsd.edu/research/posters/AHM_2011/paul_ruvulo.pdf)
57. Zhuang, Z., S. Benson, and D. Viscusi, Digital 3-D headforms with facial features representative of the current US workforce. *Ergonomics*, 2010. **53**(5): 661–671.
58. De Greef, S., et al., *Large-scale in-vivo Caucasian facial soft tissue thickness database for craniofacial reconstruction.* *Forensic Sci Int*, 2006. **159 Suppl 1**: S126–S146.
59. *MSDS: Task 9 and Task 10*, [http://www.smooth-on.com/msds/files/Task\\_9\\_10.pdf](http://www.smooth-on.com/msds/files/Task_9_10.pdf)
60. Hanson, D., *Humanlike Articulated Robotic Headform to Replace Human Volunteers in Respirator Fit Testing: Operations Manual*, AFRL-RX-TY-TP-2012-0073-02, Air Force Research Laboratory, Tyndall AFB, FL, 2012.
61. Bergman, M.S., et al., Development of an Advanced Respirator Fit Test Headform, *J. Occup. Envi. Hyg.*, submitted.

## LIST OF SYMBOLS, ABBREVIATIONS AND ACRONYMS

ABS	acrylonitrile–butadiene–styrene plastic
AFRL	Air Force Research Laboratory
BARDA	Biomedical Research and Development Authority, U.S. Department of Health and Human Services
CFR	Code of Federal Regulations
CO <sub>2</sub>	carbon dioxide
DoD	Department of Defense
FF	fit factor
FFR	filtering facepiece respirator
ID	inner diameter
IL	inward leakage
in	inch
IRP	individual respiratory protection
km	kilometer
L/min	liters per minute
mL	milliliter
mm	millimeter
MPPS	most-penetrating particle size
NIOSH	National Institute for Occupational Safety and Health
PDMS	polydimethylsiloxane
PVC	poly(vinyl chloride)
QNFT	quantitative fit testing
WWI, WWII	World Wars I, II
µm	micrometer (historically, micron)